Adsorption of Wheat protein Isolate by Hallosyte nanotubes: Kinetics and Equilibrium modeling

C. Madhavi[1], O. Sreekanth Reddy[2], G. Ujwala[2], K. S. V. Krishna Rao[3]*

[1]*Department of Polymer Science and Technology, Sri Krishnadevaraya University, Ananthapuramu, Andhra Pradesh, India,* [2]*Department of Chemistry, Sri Krishnadevaraya University, Ananthapuramu, Andhra Pradesh, India,* [3]*Department of Chemistry, Yogivemana University, Kadapa, Andhra Pradesh, India*

ABSTRACT

This study reports the adsorption of wheat protein isolate (WPI) from aqueous solution on Hallosyte nanotubes (HNT). Batch adsorption experiments were carried out as a function of pH, contact time and initial concentration of the adsorb at solution at room temperature. Kinetic data were best fit to a pseudo second order rate equation for the adsorption of WPI on HNTs. The equilibrium data better fit the Freundlich isotherm model for the adsorption of WPI on HNTs. A modified Freundlich equation was proposed, and compared with Freundlich equation. Due to the high porosity, the HNTs are accessible for protein adsorption. The material reveals high adsorption capacities for WPI at pH 7.4 and concentration of 1000 mg, where by proteins are mainly adsorbed via electrostatic interactions.

Key words: Adsorption, Wheat proteins isolate, Hallosyte nanotubes, Batch technique, Freundlich isotherm, Kinetic model.

1. INTRODUCTION

Naturally abundant clay minerals and their new hybrid materials are a class of layer edalumosilicates possessing large specific surface area, chemical and mechanical stability, high cation exchange capacity, and good biocompatibility have made the clays excellent adsorbent materials [1-3]. Over the past decades, the studies on the adsorption and binding of biomolecules, such as proteins and nucleic acids, by clay minerals play an active part in numerous fields of biomedical and nanotechnology, for example, for biosensors, biochips, and drug delivery materials [4-6]. Protein adsorption at solid-liquid interfaces can be studied through various analysis techniques [7]. Understanding the factors that dominate protein adsorption behaviors is very important for designing and synthesizing biomaterials. Thus far, many studies of protein adsorption onto various biomaterial surfaces have been carried out and adsorption mechanisms have been proposed from different aspects, such as topology structure, hydrophilicity/hydrophobicity, electrostatic interactions, and segment mobility of the surfaces [8-13].

The adsorptions of various solutes on a solid remain an active area of research. However, finding simple and easily performable experiments to illustrate the quantitative aspects of adsorption can be very difficult [14]. The common adsorbents include activated carbon, molecular sieves, polymeric adsorbents, and some other low-cost materials. Thermodynamic and kinetic studies are important aspects to know more details about adsorption performance and mechanisms. In addition to adsorption capacity, the kinetic performance of a given adsorbent is also of great important for the pilot applications [15].

The adsorption of proteins has been studied using α-zirconium phosphate adsorption of proteins and cells has been studied with montmorillonite and related layered clays [16-22]. The costs of isolation and purification of proteins form a significant part (40–80%) of the overall cost of protein production. Therefore, protein immobilization on solid surfaces of smectic clay is of particular interest. Kumar *et al.* [20] stated that proteins are sensitive to the pH and temperature

of their environment; for example, they are unstable in organic solvents. These problems can be overcome if the protein molecules are adsorbed in inorganic-layered materials which may also be employed as biocatalysts and biosensors [23,24]. Intercalation characteristics of clays, modified clays, or smectites can also be used for protecting the environment from pollutants.

Halloysite nanotubes (HNT), $Al_2Si_2O_5 (OH)_4 \cdot nH_2O$, [25] is a natural tubule material formed by rolled kaolin sheets. Surface of halloysite tubes is silica and its innermost surface is alumina, providing a strong negative zeta-potential of ca. −30 mV on the tube surface and +25 mV in the inner most surface of the tube in aqueous dispersions at normal pH, this significantly affects the protein–nanotubes interaction. The Halloysite tube's diameter is of 40–70 nm with inner lumen diameter of 10–15 nm and length of 1500 ± 500 nm. With a hollow nanotubular structure, high specific area, and high porosity, HNTs show good adsorption performance. Earlier reports have shown that HNT can be used as an efficient adsorbent for methylene blue, neutral red, methyl violet, uranium, 5-aminosalicylic acid, etc. [26] Thus, HNT is a multifunctional material with good mechanical properties, high adsorption capacity, and environmental friendly properties [27]. Due to their particular tubular structure which in safe, and biocompatible, and exhibits negative surface charges, they can be used as ion exchangers to adsorb proteins and biomolecules.

*Corresponding author:
K. S. V. Krishna Rao,
E-mail: ksvkr@yogivemanauniversity.ac.in

Wheat protein (WP), existing in various wheat products, is one of the most abundant renewable resources and is receiving burgeoning interest for non-food usage [28,29]. At present, WP is commercially available in three different forms from Wheat processing plants: Wheat flour (SF, 54% protein), WP concentrate (WPC, 65–72% protein), and WP isolate (WPI ≥90% protein). These wheat products are primarily utilized in food and as plastic components in blending polymers, or as simple fillers in various polymer matrices, to improve the mechanical properties of the polymeric systems [30]. WPI consists of about 18 kinds of amino acids, of which about 62% are polar and reactive amino acid residues, including some containing carboxyl groups and some containing amino groups. This offers an intriguing possibility for WPI and HNT adsorption or binding [31]. However, to the best of our knowledge, there has not been any reported study on the use of WPI adsorption on HNT.

In the present study, we focused on the adsorption behavior of WPI on HNTs. The effects of concentration, pH, and adsorption amount of WPI on HNT were studied. The adsorption isotherms and kinetics of the adsorption process were also investigated.

2. EXPERIMENTAL

2.1. Materials and Methods

WPI is purchased Pro-FAM 974 Isolated protein (ADM foods and Wellnes) USA. Hallosyte nanotubes (HNTs) were purchased from Natural Nano Inc., USA. NaOH was purchased from sigma Aldrich Co. USA. The chemical composition of the HNTs is shown in Table 1. Before processing, the fillers were dried in an oven at 80 ºC for 12 h to eliminate moisture. All materials were used without further purification.

2.2. Preparation of WPI Solution

The test solutions were prepared by diluting a stock solution of WPI to the desired concentrations. A stock solution of WPI was obtained by dissolving 1.0 g of WPI in aqs NaOH solution and then was diluted to 1000 mL. Several dilutions of stock solution were made at different pH to obtain the specific concentrations required for the adsorption study. 0.5 g of HNT was weighed and introduced into 250 mL conical flask. 50 mL of a 1000 mg/L solution of WPI prepared in aqs NaOH solution from the stock solution was added to the HNT. The flasks were placed in a sonication bath for 1 h. The suspensions were centrifuged for 10 min at 4000 rpm and the supernated liquied was decaned and analyzed.

2.3. Adsorption Study

Adsorption experiments were carried out by shaking 0.5 g of adsorbent (HNTs) with 50 mL of adsorbate solution of desired concentration in a 250 mL conical flask placed in a sonication bath. The solution-adsorbent mixtures were sonicated and incubated; at the end of a predetermined time interval, the reaction mixtures were centrifuged and the supernatant liquid was analyzed for WPI concentration using aUV/Vis spectrophotometer by measuring the absorbance at the wavelength of maximum absorption of 280 nm. The adsorption kinetics of the adsorbate were determined for the incubated the samples after the desired contact time by measured the remaining unadsorbed concentration. The same procedure was used to study the effect of contact time (5–100 min), initial WPI concentrations

(100–1000 mg/L), adsorbent amount (0.1–0.7 g/50 mL solution), and pH (7.4–10).

All experiments were carried out in triplicate, and the concentrations given are average values. The initial concentration in the test solution and the adsorbent dosage were varied to investigate their effect on the adsorption kinetics. The adsorption studies were carried out at room temperatures. The amount of adsorption at time t, q_t (mg/g), was calculated using the following equation:

$$q_t = \frac{(C_o - C_t)V}{M} \qquad (1)$$

Where C_0 is the is the initial value of the protein concentration in the solution, C_t is the liquid phase concentration (mg/mL) at any time, V is the volume of the protein solution (L) and M is the mass of dry adsorbent (g). The amount of adsorption at equilibrium, q_e (mg/g) was computed as follows:

$$q_t = \frac{(C_o - C_t)V}{M} \qquad (2)$$

Where C_o and C_e are the initial and final (equilibrium) concentrations of SPI (mg/L), respectively.

3. RESULTS AND DISCUSSION

3.1. Effect of Contact Time and Concentration

To find the time for equilibrium adsorption at room temperature, the contact time of WPI on HNT was varied from 5 to 100 min at different WPI concentrations, with the amount of adsorbent of 0.5 g/50 mL solution, agitation for 1hr, for three different pH values are shown in Figure 1a-c. It was found that in the initial stage, the adsorption curve rose sharply with time, indicating that the rate of adsorption of WPI was high, and that there were plenty of readily accessible sites [32]. At pH 7.4 and 1 g/50 mL, the adsorption reaches a maximum at 34.00 mg/g at 60 min and then remained unchanged with further elapse of time. Hence, the optimum contact was chosen as 60 min. It was also clearly indicated that the adsorbed quantity of protein increased as the protein solution concentration increased, with the equilibrium also increasing; this adsorption behavior may be influenced by the ionic strength of the HNTs, charge density, and protein-protein lateral repulsion in the HNTs. Furthermore, at high concentration, the surface will be occupied in a shorter time sequence and the time for spreading will be shorter. As a consequence, the adsorbed concentration will be larger. An adjustment of the surface negative charge density of the HNT may even increase the amount of adsorbed protein molecules as well as the density of the protein molecules per unit area on the tube surface [4].

3.2. Adsorbent Amount

The effect of adsorbent amount (HNT) on the absorption of WPI is shown in Figure 2; The adsorption of WPI gr HNT decreased with increasing amount of HNT (0.1–0.7 g/50 mL solution) at a constant WPI concentration of 1000 mg/L, contact time 60 min, agitation for 1 h, and pH of 7.4 at room temperature. This can be attributed to an increased adsorbent surface area and availability of more adsorption sites resulting from the increased adsorbent amount [33,34]. With the increase in adsorbent amount, the adsorption capacity decreased

Table 1: Chemical compositions of natural Hallosyte nano tubes.

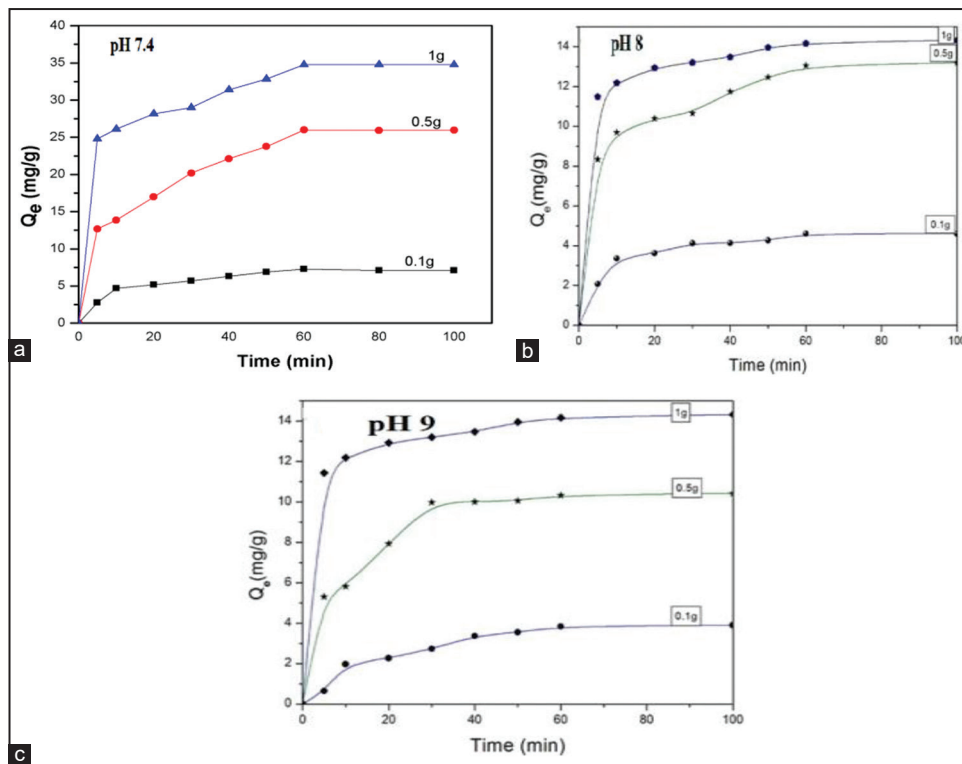| Chemical composition	SiO$_2$	Al$_2$O$_3$	Fe$_2$O$_3$	K$_2$O	TiO$_2$	CaO+MgO	Ignition
Weight %	40	34	3.5	0.5	1	2.5	17.5

Figure 1: Effect of contact time on adsorption at (a) pH 7.4, (b) pH 8, and (c) pH 9.
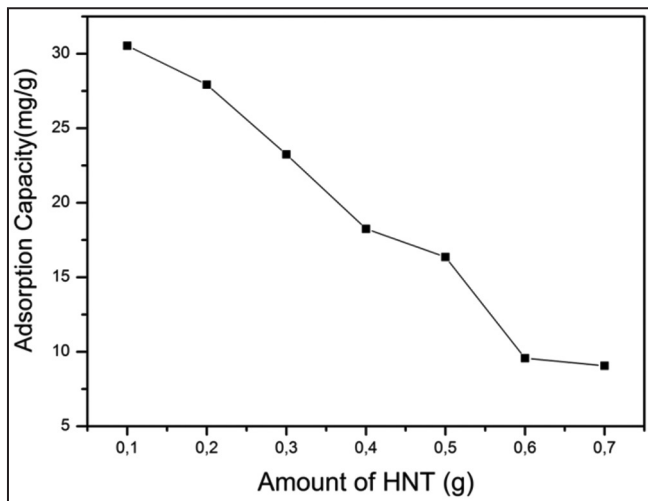

Figure 2: Effect of absorbent amount on adsorption of WPI onto HNT (Initial concentration Of WPI = 1000 mg/L, pH = 7.4, contact time = 60 min, agitation time for 1hr and at room temperature).
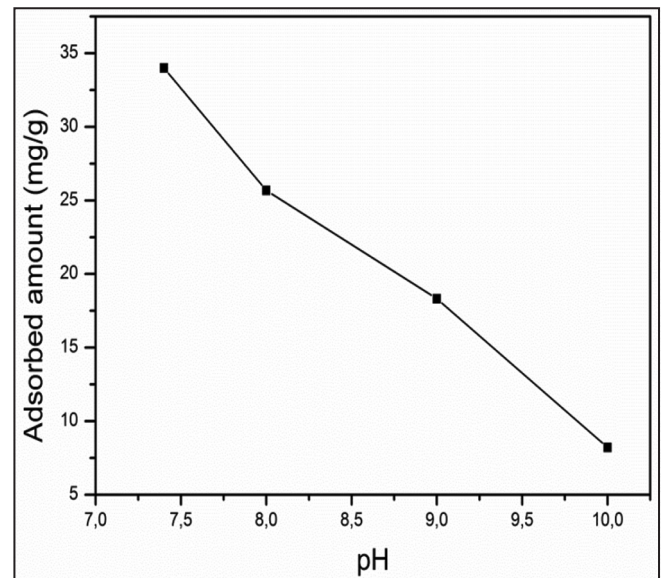

Figure 3: Effect of pH on adsorption of SPI onto HNT.

from 30.54 to 9.06 mg SPI/g HNT. With 0.5 g of HNT Above this amount (0.5 g HNT per 50 mL solution), the adsorption of WPI attains equilibrium.

3.3. Effect of pH

The pH of the solution affects the surface charge of the adsorbents, ionization, rate of adsorption, and dissociation of functional groups. The effect of pH on the adsorption of WPI was studied by varying the pH from 7.4 to 10 and is plotted in Figure 3. The maximum (equilibrium) uptake of adsorbate was the highest at a pH of 7.4, with the adsorption capacity of 34 mg/g of HNT. The WPI used in this study contained amine and carboxyl groups which were protonated or deprotonated depending on the pH of the solution. The adsorption of WPI is mainly influenced by the amount of negative charges in the solution which is, in turn, influenced by the solution pH. At higher pH, there is a net positive charge in the solution so adsorption is less, whereas at lower pH (7.4), there was increase in negative charges increasing the adsorption of WPI. The maximum adsorption was found to take place at pH 7.4, the lowest pH was used. However, it was not close to zero, as it should be ideally. As it should be ideally. The following reasons may explains this behavior: (1) The interactions between WPI and the surfaces, including the edges of the tubes, cannot be completely induced by pure electrostatics; hydrogen-bonding due to the form of hydroxyl groups and van der Waals interactions should also contribute. (2) The concentrations of WPI/HNTs were too high.

3.4. Adsorption Isotherms

To describe the isotherms [Figure 4], Langmuir and Freundlich models were used; details of the model equations are given in Table 2. Values of the correlation coefficients and other parameters are summarized in Table 3. Normally, for the estimation of best fit, the values of correlation coefficients (R^2) of linear plots of the different models are considered. Figure 5a-e show exemplary the adsorption of WPI fitted with the Langmuir equation and the Freundlich equation, respectively; the fits to the measured data for both equations can be noticed. The regression coefficients, R^2, values for the Freundlich equation used
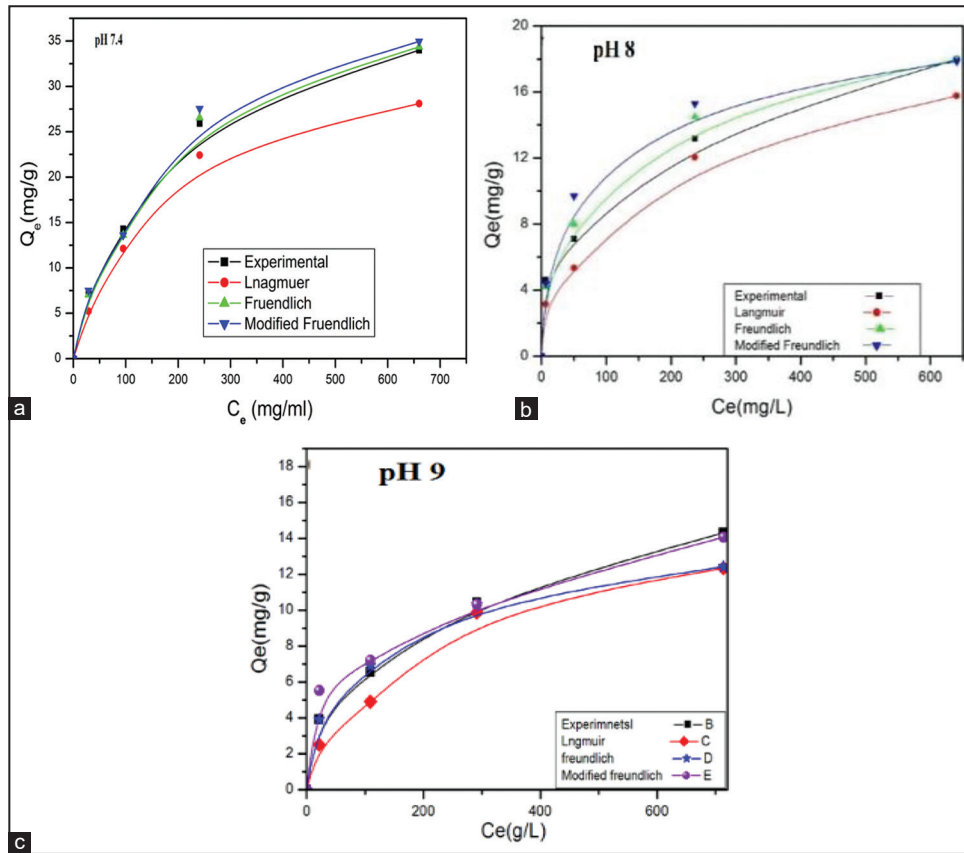

Figure 4: Adsorption isotherms of WPI adsorption on HNT at (a) pH 7.4, (b) pH 8, and (c) pH 9.

Table 2: Equilibrium model equationsm, slope and intercept for the isotherm Equations [31].

Model Isotherm	General form	Linear form	Plot	Slope	Intercept
Langmuir		$Q_e = \dfrac{Q_m K_L C_e}{1 + K_L C_e} \quad \dfrac{C_e}{q_e} = \dfrac{1}{Q_m} Ce + \dfrac{1}{K_L Q_m} \dfrac{C_e}{q_e}$ vs C_eSlope $= \dfrac{1}{Q_m}$ Intercept $= \dfrac{1}{K_L Q_m}$			
Freundlich		$Q_e = K_M Ce^{\frac{1}{n_F}} \quad \ln(Qe) = \ln(K_F) + \dfrac{1}{n_F} \ln(Ce) / n(C_e)$ vs $\ln(Q_e)$ Slope $= \dfrac{1}{n_F}$ Intercept $= \ln K_F$			
Modified Freundlich		$Q_e = K_{MF} Ce^{\left(\frac{1}{n_{MF}} - 1\right)} \quad \ln\left(\dfrac{Qe}{Ce}\right) = \ln(K_{MF}) + \left(\dfrac{1}{n_{MF}} - 1\right) \ln(Ce)$ Slope $= \dfrac{1}{n_F} - 1$ Intercept $= \ln K_{MF}$			

C_e=dye concentration at equilibrium (mg L^{-1}); Q_e=equilibrium adsorption capacity (mg g^{-1}); K_L=Langmuir adsorption constant (L mg^{-1}); Q_m=maximum adsorption capacity (mg g^{-1}); K_F=Freundlich constant (L g-1); n_F=heterogeneity factor of adsorption sites (dimensionless). K_{MF}=modified Freundlich constant (L g^{-1}); n_{MF}=heterogeneity factor of the adsorbent sites (dimensionless)

Table 3: Correlation coefficients and constant parameters calculated forvarious adsorption models at different pH for WPI pH.

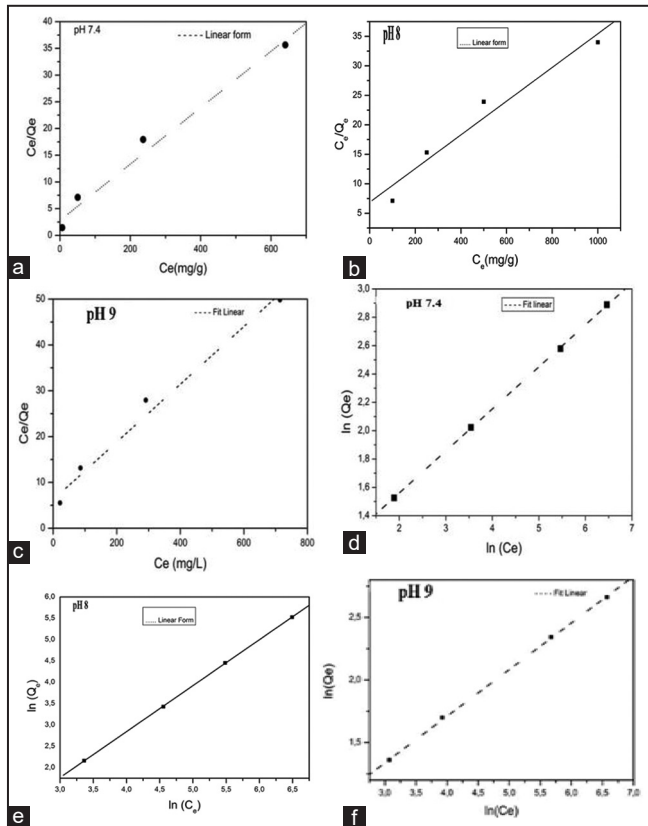| Parameter	7.4	8	9
Langmuir			
R^2	0.98106	0.97697	0.98079
Qm (mg/g)	1.81	0.14	0.16
KL (L/mg)	2.54	2.40	0.36
Freundlich			
R2	0.99995	0,99997	0.99992
nF	3.36	2.95	2.68
KF (L/g)	9.98	1.305	3.62
Modified Freundlich			
R20.99997	0.99996	0.99995	
nMF	3.36	2.95	2.68
KMF (L/g)	9.98	1.305	3.62

Figure 5: Linear fit for adsorption isotherms of WPI. (a) Linear form at ph 7.4 (b) Linear form at 8 (c) Linear form at 9 (d) Freundlich asorption isotherm at ph 7.4 (e) Freundlich asorption isotherm at 8 (f) Freundlich asorption isotherm at 9.

was near unity. The agreement with the experimental data, especially to the Freundlich isotherm, implies the existence of different adsorption energies on the nanotube surface. It may be due to the protein adsorption taking place in a monolayer (chemisorption) adsorption, but also multilayer (physisorption) adsorption by lateral interactions between the adsorbate molecules may be imaginable. Therefore, the Freundlich model is suggested for adsorption of WPI by the HNT.

Plots of $\ln(Q_e/C_e)$ vs. $\ln(C_e)$ showed a linear relation [Figure 6] with values of R^2 near to unity for both pH. The values were found to be identical with those calculated by the Freundlich equation. The linear equation obtained for the new model from this relation is shown in Figure 6. Values of adsorption calculated using K_{MF} and n_{MF}th the linear and nonlinear forms of a new equation were found to be identical. These results showed the validity of the non-linear form of the equation. This equation is similar to the Freundlich equation and has been designated as the modified Freundlich equation. Values of parameters, K_{MF} and n_{MF}, calculated using the modified Freundlich equation isotherms, were identical with those of values calculated using the Freundlich equation. The values of R^2 of the linear plots of HNT were better than those of the Langmuir and Freundlich models. This indicated that the modified Freundlich equation can be used in place of the Freundlich equation which showed better fit with respect to the values of the correlation coefficient, R^2.

3.5. Adsorption Kinetic Studies

The adsorption of proteins as ionic species to charged surfaces involves chemisorption as the controlling step in the dynamics of the adsorption process. The models were implemented to analyze the experimental data of protein adsorption [35-40].

3.5.1. Pseudo-first order

Pseudo-first-order equation

$$\frac{dQ_e}{dt} = k_1(Q_e - Q_t) \tag{3}$$

The linearized form of the pseudo-first-order equation is generally expressed as follows:

$$\ln(Q_e - Q_t) = \ln Q_e - k_1 t \tag{4}$$

Where Q_e is the amount of WPI adsorbed at equilibrium (mg adsorbate/g adsorbent), Q_t is the amount of WPI adsorbed at time t (mg adsorbate/g adsorbent), k_1 is the first-order rate constant (min^{-1}) and t is time in (min). If a plot of $\ln(Q_e–Q_t)$ against time t at different pH gives a linear relationship, the pseudo-first-order rate constant (k_1) and equilibrium adsorption capacity (Q_e) can be calculated from the slope and intercept, respectively, they are given in Table 4 for the three pH values.

3.5.2. Pseudo-second order

The kinetic rate expression for a pseudo-second-order model (eq (5)) and linearized (eq (6)) form its was applied to the experimental data.

$$\frac{dQ_e}{dt} = k_2(Q_e - Q_t)^2 \tag{5}$$

$$\frac{t}{Q_t} = \frac{1}{k_2 Q_e^2} + \frac{t}{Q_e} \tag{6}$$

Here Q_t is the amount of WPI molecules on the HNT surface (mg adsorbate/g adsorbent) at time t, Q_e is the amount (mg adsorbate/g adsorbent) of WPI adsorbed at equilibrium, k_2 is the pseudosecond-order rate constant (g adsorbent/mg adsorbate/min). The slope and intercept of at/(Q_t) vs. t plot gives ho and k_2, which are shown in Table 2 for different pH.

From Table 4, the values of the correlation coefficient, R^2 for the adsorbents were near to unity, then closer for the pseudo first order model, and that calculated Q_e values matched well with the experimental value, demonstrating that adsorption of WPI followed a pseudo second order rate expression. These kinetic models are same as our earlier studies.
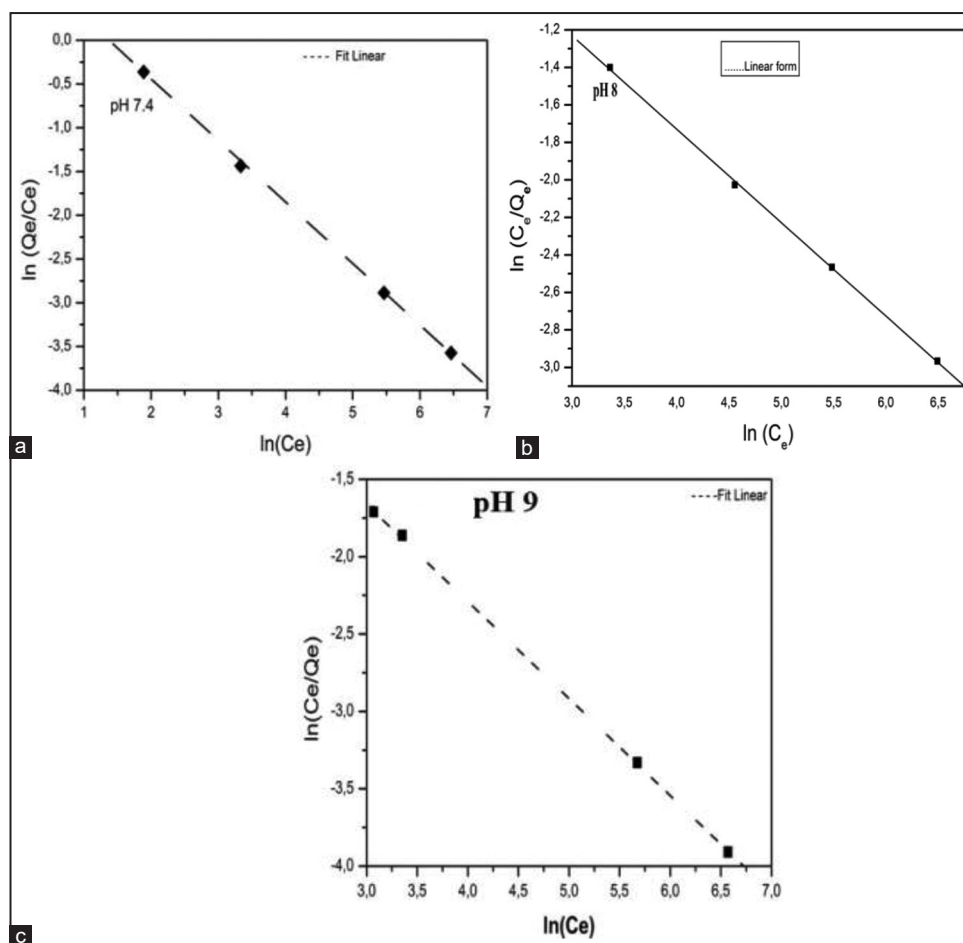
Figure 6: Linear fit for the modified Freundlich model for the adsorption of WPI at different pH on HNT.

Table 4: Pseudo-first-order kinetic model.

pH	C_0 (mg/g)	Qeexp (mg/g)	Qecal 5/mim	K_1	R^2
9	100	0.64	0.27	0.04955	0.97645
	500	5.31	2.29	0.04519	0.97448
	1000	11.43	9.29	0.04402	0.98575
8	100	2.08	1.33	0.05149	0.98203
	500	8.33	5.73	0.04325	0.96205
	1000	14.05	10.55	0.0405	0.9825
7.4	100	7.11	6.33	0.08325	0.97305
	500	25.91	20.45	0.07952	0.98309
	1000	34.00	28.22	0.05431	0.9843

4. CONCLUSIONS

This study investigated the adsorption of WPI from an aqueous solution with HNT by batch experiment method. The adsorption was found to be strongly influenced by pH, contact time, and temperature. The adsorption was pH dependent, with the adsorption capacity maximum at pH 7.4. Equilibrium was attained at 60 min. The Langmuir and Freundlich isotherm models were tested and model parameters were estimated. The overall data were better fitted by Freundlich isotherm at room temperature range surface of the HNT is likely capable of inducing multilayer adsorption. The pseudo-second-order kinetic model was found to be the best fit for the adsorption of WPI on HNT.

A modified Freundlich equation has been suggested, which gave values of all the parameters identical to those of the Freundlich model, but with values of R^2 closer to one and better than the Langmuir model. On the basis of these results, it can be concluded that the Freundlich equation should be replaced by the modified Freundlichsice it gave better values of R^2 than that of the Freundlich, but with identical values of other Freundlich parameters.

5. REFERENCES

1. W. H. Li, D. S. Tong, C. H. Zhou, C. X. Lin, C. Y. Xu, (2013) Adsorption of proteins and nucleic acids on clay minerals and their interactions: A review, *Applied Clay Science*, **80**-81: 443.

2. Y. Liu, N. Wang, J. H. Pan, F. Steinbach, J. Caro, **(2014)** *In situ* synthesis of MOF membranes on ZnAl-CO₃ LDH buffer layer-modified substrates, *Journal of American Chemical Society*, **136:** 14353-14356.

3. K. Rall, U. Sohling, D. Riechers, C. Kasper, F. Ruf, T. Scheper, (2010) Adsorption and separation of proteins by a smectitic clay mineral, *Bioprocess Biosystem Engineering,* **33:** 847-861.

4. V. W. Chao(Wu), C. C. Hsu, W. M. Lu, W. J. Chen, B. Naveen, T.Y. Tsai, (2015) Protein-concentration-dependent adsorption behavior of inorganic layered materials, *Royal Society of Chemistry*, **5:** 10936.

5. P. Mignon, M. Sodupe, (2012) Theoretical study of the adsorption of DNA bases on the acidic external surface of montmorillonite, *Physical Chemistry Chemical Physics*. **14:** 945.

6. Q. Wang, D. O'Hare, (2012) Recent advances in the synthesis

and application of layered double hydroxide (LDH) nanosheets, *Chemical Reviews*, **112:** 4124-4155.

7. M. V. Manso, A. G. Ceccone, F. Rossi, (2004) Activation of PCL surface by ion beam treatment to enhance protein adsorption, *Journal of Bioactive and Compatable Polymers*, **19:** 287.

8. Y. Dahman, K. E. Jayasuriya, (2013) Preliminary study of binary protein adsorption system and potential bioseparation under homogeneous field of shear in airlift biocontactor, *Advances in Bioscience and Biotechnology*, **4:** 710-718.

9. J. Ndor, N. Orgovan, M, Fried, P. Petrik, A. Sulyok, J.J. Ramsden, L. Korosi, R. Horvath, (2014) Enhanced protein adsorption and cellular adhesion using transparent titanate nanotube thin films made by a simple and inexpensive room temperature process: Application to optical biochips, *Colloids and Surfaces B: Biointerfaces,* **122:** 491-497.

10. G. Rangel-Porras, P. Rangel-Rivera, H. Pfeiffer-Pereab, P. Gonzalez-Muñoza, (2015) Changes in the characteristics of acid-treated clay after the inclusion of proteins, *Surface and Interface Analysis*, **47:** 135-141.

11. A. Tran, B. James, (2012) Study the interaction forces between the bovine serum albumin protein and montmorillonite surface, *Colloids and Surfaces A: Physico Chemical Engineering Aspects,* **414:** 104-114.

12. N. Welsch, Y. Lu, J. Dzubiella, Ballauff M, (2013) Adsorption of proteins to functional polymeric nanoparticles. *Polymer,* **54:** 2835-2849.

13. H. Ayhan, (2002) Model protein BSA adsorption and covalent coupling onto methyl methacrylate based latex particles with different surface properties, *Journal of Bioactive and Compatible Polymer,* **17:** 271.

14. M. T. Uddin, M. S. Islam, M. Z. Abedin, (2007) Adsorption of phenol from aqueous solution by water hyacinth ash. *ARPN Journal of Engineering Applied Science,* **2**: 121.

15. H. Qiu, L. Lv, B. C. Pan, Q. J. Zhang, W. M. Zhang, Q. M. Zhang, (2009) Critical review in adsorption kinetic models, *Journal of Zhejiong University Science A,* **10:** 716-724.

16. R. D. Misra, C. Nune, (2014) Biological response to self-assembly of preadsorbed proteins at biointerfaces: Significance, cellular activity and perspective, *Material and Technology*, **29**: B41-B48.

17. R. D. Misra, C. Nune, T. C. Pesacreta, M. C. Somani, L. P. Karjalainen, (2013) Understanding the impact of grain structure in austenitic stainless steel from a nanograined regime to a coarse-grained regime on osteoblast functions using a novel deformation-annealing sequence, *Acta Biomaterials,* **9:** 6245-6248.

18. C. Nune, R. D. Misra, M. C. Somani, L. P. Karjalainen, (2014) Dependence of cellular activity at protein adsorbed biointerfaces with nano-to microscale dimensionality, *Journal of Biomedical Material Research Part: A*. **102:** 1663-1676.

19. K. C. Nune, R. D. Misra, (2014) Pre-adsorption of protein on electrochemically grooved nanostructured stainless steel implant and relationship to cellular activity, *Journal of Biomedical Nanotechnology*, **10:** 1320.

20. C. V. Kumar, G. L. McLendon, (1997) Nanoencapsulation of cytochrome c and horseradish peroxidase at the galleries of α-zirconium phosphate, *Chemistry of Materials*, **9:** 863-870.

21. C. Salvador-Morales, E. Flahaut, E. Sim, J. Sloan, M. L. Green, R. B. Sim, (2006) Complement activation and protein adsorption bycarbon nanotubes, *Molecular Immunology*, **43:** 193-201.

22. J. J. Lin, J. C. Wei, T. Y. Juang, W. C. Tsai, (2007) Preparation of protein-silicate hybrids from polyamine intercalation of layered montmorillonite, *Langmuir*, **23:** 1995-1999.

23. C. Mousty, (2004) Sensors and biosensors based on clay-modified electrodes-new trends, *Applied Clay Science*, **27:** 159-177.

24. E. Abdullayev, A. Joshi, W. Wei, Y. Zhao, Y. Lvov, (2012) Enlargement of halloysite Clay nanotube lumen by selective etching of aluminum oxide, *ACS Nano*, **6:** 7216-7226.

25. L. Jiang, C. Zhang, J. Wei, W. Tjiu, J. Pan, Y. Chen, T. Liu, (2014), Surface modifications of halloysite nanotubes with superparamagnetic Fe_3O_4 nanoparticles and carbonaceous layers for efficient adsorption of dyes in water treatment, *Chemical Research in Chinese Universities,* **30:** 971-977.

26. H. J. Choi, T. J. Stazak, C. D. Montemagno, (2013) Surface-dependent cytotoxicity on bacteria as a model for environmental stress of halloysite nanotubes, *Journal of Nanopartical Research*, **15:** 13.

27. J. Y. Ji, B. Li, W. H. Zhong, (2014) An ultra elastic poly(ethylene oxide)/soy protein film with fully amorphous structure, *Macromolecules*, **45:** 602.

28. F. Song, D. L. Tang, X. L. Wang, Y. Z. Wang, (2011) Biodegradable soy protein isolate-based materials: A review, *Biomacromolecules,* **12:** 3369.

29. J. Y. Ji, B. Lively, W. H. Zhong, (2012) Soy protein-assisted dispersion of carbon nanotubes in a polymer matrix, *Material Express*, **2:** 76.

30. E. Logakis, C. H. Pandis, P. Pissis, J. Pionteck, P. Pötschke, (2011) Highly conducting poly (methyl methacrylate)/carbon nanotubes composites: Investigation of their thermal, dynamic-mechanical, electrical and dielectric properties, *Composites Science and Technology,* **71:** 854-862.

31. A. S. Bhatt, P. L. Sakaria, V. Manu, R. R. Pawar, N. Sudheesh, H. C. Bajaj, H. M. Mody, (2012) Adsorption of an anionic dye from aqueous medium by organoclays: Equilibrium modeling, kinetic and thermodynamic exploration, *RSC Advances*, **2:** 8663.

32. M. T. Uddin, M. S. Islam, M. Z. Abedin, (2007) Adsorption of phenol from aqueous solution by water hyacinth, *ARPN Journal of Engineering Applied Science*, **2**: 11-17.

33. F. A. Banat, B. Al-Bashir, S. Al-Asheh, O. Hayajneh, (2000) Adsorption of phenol by bentonite, *Environmental Pollution*, **107:** 391-398.

34. V. C. Srivastava, M. M. Swammy, I. D. Mall, B. Prasad, I. M. Mishra, (2006) Adsorptive removal of phenol by bagasse fly ash and activated carbon: Equilibrium, kinetics and thermodynamics, Colloids Surfaces A: Physico *Chemical* Engineering *Aspects*, **272:** 89-104.

35. K. R. Hall, L. C. Eagleton, A. Acrivos, T. Vermeulen, (1966) Pore-and solid-diffusion kinetics in fixed-bed adsorption under constant-pattern conditions, *Industrial and Engineering Chemistry Fundamentals*, **5:** 212-223.

36. M. J. Reddy, T. J. Vani, N. S. Reddy, K. S. Rao, P. N. Kumar, L. K. Reddy, A. V. Reddy, (2013) The synergistic extraction of uranium with mixtures of cyanex-272 and cyanex-923, TPBD, TNBD, TOPO from thiocyanate medium, *Indian Journal of Advances in Chemical Science,* **1(2)**: 99-104.

37. N. S. Reddy, K. S. Rao, K. M. Rao, S. Parambadath, C. S. Ha, (2016) Aminothiozolyl maleamic acid based multi chelating hydrogels for the separation of uranium (VI) ions from aqueous environment, *Polymers for Advanced Technologies*, **27(10)**: 1317-1324.

38. N. S. Reddy, K. M. Rao, T. J. Vani, K. S. Rao, Y. I. Lee, (2016) Pectin/poly (acrylamide-co-acrylamidoglycolic acid) pH

sensitive semi-IPN hydrogels: Selective removal of Cu2+ and Ni2+, modeling, and kinetic studies, *Desalination and Water Treatment*, **57(14)**: 6503-6514.

39. T. J. Vani, N. S. Reddy, P. R. Reddy, K. S. Rao, J. Ramkumar, A. V. Reddy. (2014) Synthesis, characterization, and metal uptake capacity of a new polyaniline and poly (acrylic acid) grafted sodium alginate/gelatin adsorbent, *Desalination and Water Treatment,* **52:** 526-535.

40. T. J. Vani, N. S. Reddy, K. S. Rao, P. S. Rao, (2016) Development of novel blend membranes based on carbohydrate polymers for the removal of toxic metal ions through sorption, *Desalination and Water Treatment*, **53:** 25729-25738.

Bibliographical Sketch

Dr. C. Madhavi is presently working as Academic consultant in the Department of Polymer Science and Technology, S. K. University, Anantapur. She obtained his MSc and PhD degrees in Polymer Science and Technology, (area of research is Drug delivery studies) from S. K. University. She has been in the teaching field for the past 6 years. She has more than 30 research publications to her credit, published in national and international journals. He has presented 5 papers in various seminars.